

Protein Surface Interactions Probed by Magnetic Field Effects on Chemical Reactions

Kiminori Maeda,^{*,†,‡} Alexander J. Robinson,[‡] Kevin B. Henbest,[‡] Emma J. Dell,[‡] and Christiane R. Timmel^{*,†,‡}

Centre for Advanced Electron Spin Resonance and Inorganic Chemistry Laboratory, Department of Chemistry, University of Oxford, Oxford OX1 3TA, U.K.

Received October 28, 2009; E-mail: kiminori.maeda@chem.ox.ac.uk; christiane.timmel@chem.ox.ac.uk

Detection of spin polarization in photochemically produced radical pairs embedded within or on the surface of proteins by chemically induced dynamic nuclear or electron polarization (CIDNP or CIDEP) has proven very valuable in unraveling both protein binding and protein folding processes.^{1,2} However, observations of the effects that even weak static magnetic fields should exert on the yield and/or kinetics of such protein-based radical pair (RP) reactions are rare.^{3–5} Here we have exploited the magnetic field dependence of RPs created photolytically from anthraquinone-2,6-disulfonate (AQDS) and tryptophan (Trp) residues of hen egg white lysozyme (HEWL) and bovine serum albumin (BSA) to provide detailed insights into the binding properties of AQDS with these proteins.

Pulsed laser excitation of an aqueous solution of AQDS²⁻ and HEWL initially produces ^SAQDS^{2-*}, which undergoes fast inter-system crossing (ISC) to ^TAQDS^{2-*}, which in turn, via rapid electron (and proton) transfer and under conservation of total spin angular momentum, produces the triplet state of the RP, [^TAQDS^{3-*} Trp*]^{6,7} (Figure 1A). Proof of this assignment of the RP precursor and the radicals is provided by the time-resolved transient absorption (tr-TA) spectra observed following the laser pulse (at time $t = 0$) obtained at zero applied magnetic field (Figure 1B). Two pronounced bands at 400 and 520 nm due to AQDS^{3-*} radical absorption concomitant with some (smaller) contribution from Trp(H⁺)^{*} in the HEWL molecule were observed. According to CIDNP studies,⁸ the Trp* signal can be assigned to the exposed tryptophan residues, Trp123 and 62. The decay kinetics of the peaks at 400 and 520 nm were very similar and fit a double-exponential function with time constants of 0.9 and ~ 5 μ s, corresponding to geminate recombination and reaction termination, respectively. Application of an external magnetic field (45.6 mT) significantly changed the TA signal, as exemplified by the two highlighted graphs in Figure 1B at 520 nm. The rise in TA signal in the presence of an applied magnetic field corresponds to an increase in the concentration of Trp*, in accordance with the radical-pair mechanism (RPM):⁹ the generation of a pair of spin-correlated radicals in either a singlet (S) state (opposing spins) or, as here, a triplet (T) state (parallel spins) is followed by hyperfine-coupling-induced S–T interconversion, the efficiency of which can be affected by oscillating and/or static magnetic fields. Typically, only the singlet RPs are able to recombine, yielding the ground state of the molecular precursor, while the T pair is unreactive. Application of a static field whose magnitude just exceeds that of the RP hyperfine couplings¹⁰ leads to a decrease in S–T mixing efficiency and consequently, for T-born RPs, an increase in radical concentration, as observed in Figure 1B.

Figure 1C shows the effect of the magnetic field on the tr-TA, defined as $\Delta\Delta A(B, t) = \Delta A(B, t) - \Delta A(B = 0, t)$, i.e., the difference in TA signal in the presence and absence of an applied magnetic field B . Since $\Delta\Delta A$ contains contributions only from the magnetically affected species, i.e., the radicals (geminate and F-pairs) and their products, the features in Figure 1C (monotonic fall of the absorption at 400 nm, identical ratio of the peaks at 400 and 520 to that in Figure 1B) prove that the RP's precursor, ^TAQDS^{2-*}, whose absorption band strongly overlaps with that of the AQDS^{3-*} radical,¹¹ does not contribute to the TA spectra in Figure 1B. The results clearly show that quenching of ^TAQDS^{2-*} is faster than the observation time scale for [HEWL] = 0.1 mM. Previous time-resolved electron paramagnetic resonance (tr-EPR) work showed the production of TrpH⁺ (absorption at 600 nm) by primary electron transfer with ^TAQDS^{2-*}, while the data in Figure 1 support deprotonation on the submicrosecond time scale, in agreement with Kiryutin et al.⁶ The quantity

$$\text{MFE} = \frac{1}{t_2 - t_1} \int_{t_1}^{t_2} \frac{\Delta\Delta A(B, t)}{\Delta A(0, t)} dt$$

which describes the magnetic field effect on the radical yield, is plotted in Figure 2A as a function of both applied magnetic field and time after the laser flash. At the earliest times, the MFE rises most sharply between 2 and 10 mT, while the MFE for times exceeding 1 μ s is still not saturated at 45 mT. For the blue curve (0.2–0.6 μ s), the magnetic field at which the MFE reaches half its maximum value, $B_{1/2} = 8$ mT, exceeds the theoretically predicted value by a factor of nearly 2, indicating slow spin dynamics, as is usually observed for long-lived, T-born RPs in micelles or biradicals. This characteristic time evolution of the MFE can be explained by spin relaxation [see the Supporting Information (SI)]. To further explore the time dependence of this system, we examined the time profiles of $\Delta\Delta A(B, t)$ at a number of field strengths (Figure 2B). It is obvious that the graphs are not proportional to each other and attain their maximum values at different times after the laser flash. Optical inspection of the decay traces in Figure 2B shows that the RP has a lifetime of the order of microseconds, a conclusion confirmed by a more rigorous treatment of the complex kinetic model presented in the SI. In order to identify the importance of the Coulomb forces in the AQDS–HEWL interaction, we investigated the salt effect on the MFE (Figure 2C). There is clearly a striking resemblance between panels A and C of Figure 2 (i.e., between the dependences of the MFE on time and salt concentration), indicating that the RP lifetime becomes shorter as the ionic strength of the solution increases, a trend confirmed by the time profiles $\Delta\Delta A(45.6 \text{ mT}, t)$ shown in Figure 2D. In the absence of salt, $\Delta\Delta A(45.6 \text{ mT}, t)$ increases according to the difference in geminate recombination with and without the application of a field

[†] Centre for Advanced Electron Spin Resonance.

[‡] Inorganic Chemistry Laboratory.

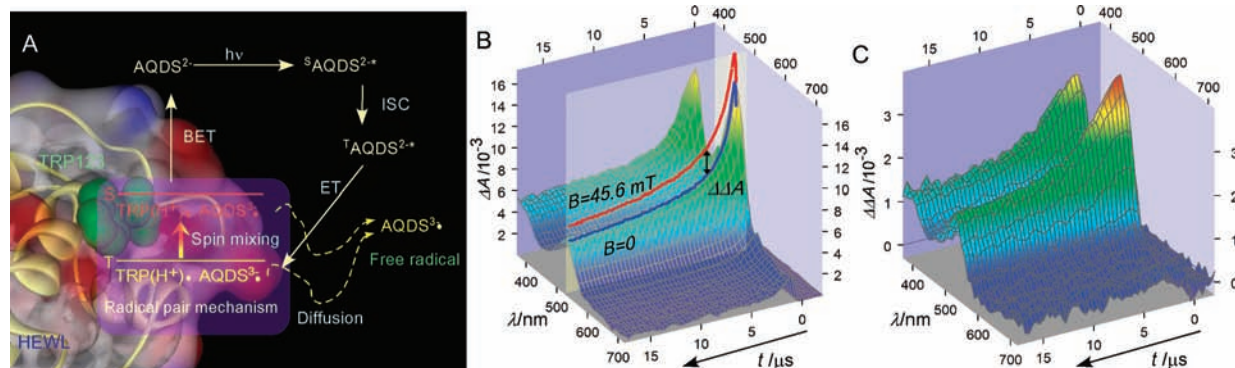


Figure 1. (A) Reaction scheme (for more details, see the text). (B) tr-TA spectra observed by laser flash photolysis (355 nm) in an aqueous solution of AQDS (0.1 mM) and HEWL (0.1 mM). The bold blue and red lines indicate the TA decay traces at 520 nm in the absence and presence (45.6 mT) of a magnetic field, respectively. (C) The difference in the tr-TA signals $\Delta\Delta A(B = 45.6 \text{ mT}, t)$ in the presence and absence of an applied magnetic field. ET, electron transfer; BET, back electron transfer.

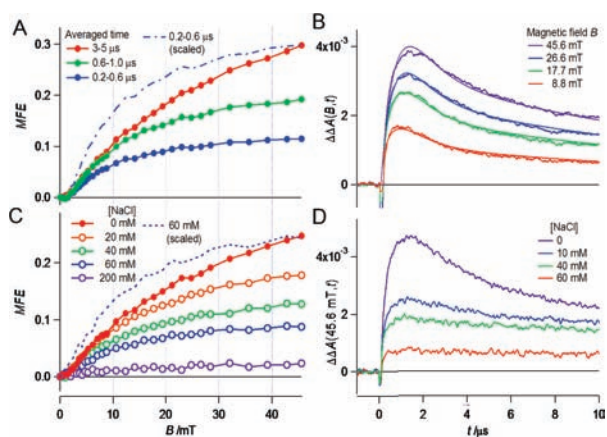


Figure 2. Flash photolysis data for aqueous solutions of AQDS and HEWL. (A) MFEs obtained by averaging tr-TA data for various time windows after the laser flash. Solid circles, raw data; dot-dashed line, 0.2–0.6 μs data rescaled to the maximum of the red curve, as shown. (B) Time profiles $\Delta\Delta A(B, t)$ for various magnetic fields. The solid lines are fitted curves (see the SI). (C) MFEs as functions of applied field: Open circles, various $[\text{NaCl}]$ as labeled; solid red circles, $[\text{NaCl}] = 0 \text{ M}$; dashed line, 60 mM data rescaled to the red-curve maximum. The integration window was 6–14 μs . (D) Time profiles $\Delta\Delta A(45.6 \text{ mT}, t)$ for various $[\text{NaCl}]$.

and then decays starting at $\sim 2 \mu\text{s}$ because of geminate recombination via spin relaxation processes. When $[\text{NaCl}] = 60 \text{ mM}$, free radicals are formed within 1 μs , and no decay component due to spin relaxation was observed because the radicals separate faster than they relax. The addition of salt decreased the MFE remarkably, indicating that the Coulomb force is the origin of the unusually large MFE.⁵ This interpretation is supported further by the fact that replacement of AQDS by the singly charged, somewhat smaller anthraquinone-2-sulfate (AQS) reduced the MFE in the absence of salt 4-fold, to 6% (results not shown). The results imply that the positive charge on the surface of HEWL increases the RP lifetime because of the attractive Coulomb force between the protein and AQDS, in agreement with previous findings.⁵ The total charge of HEWL at neutral pH is positive (isoelectric point 11.4), with the positively charged Arg residues 125 and 128 close to Trp 123 and Arg 73, 112, and 114 surrounding Trp 62.

The tr-TA spectra for BSA/AQDS are similar to those for HEWL/AQDS (see the SI), but the field and salt dependences of the $\Delta\Delta A(B, t)$ spectra are surprisingly different. Comparison of Figures 2B and 3A shows that $\Delta\Delta A(B, t)$ at 10 μs had decayed considerably for all fields applied in the BSA system, while in HEWL, a significant amount of free radicals was still present.

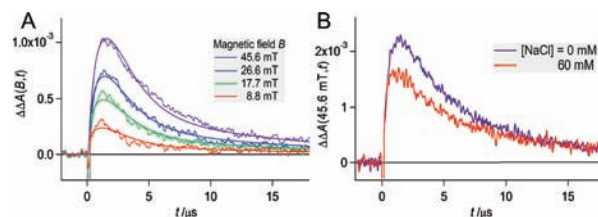


Figure 3. Flash photolysis data for aqueous solutions of AQDS and BSA. (A) Time profiles $\Delta\Delta A(B, t)$ for various magnetic fields. The solid lines are fitted curves (see the SI). (B) Time profiles $\Delta\Delta A(45.6 \text{ mT}, t)$ for $[\text{NaCl}] = 0$ and 60 mM.

Equally in contrast to the HEWL/AQDS system, addition of salt affected the BSA/AQDS tr-TA data to a far lesser degree (Figure 3B). Only the intensity is slightly diminished, indicating that the RP dynamics depend little on the solution's ionic strength. These results support the model that the AQDS molecule and hence the resulting RP are embedded within the protein and thus inert toward any change of the solvent's ionic strength.

In summary, this study proves that even weak static magnetic fields, easily produced in any laboratory, can serve as a powerful tool in investigating protein–substrate interactions.

Acknowledgment. We thank the EPSRC and the EMF Biological Research Trust for financial support and Professor Peter Hore for useful discussions.

Supporting Information Available: Full experimental details and spectral simulations. This material is available free of charge via the Internet at <http://pubs.acs.org>.

References

- (1) Kaptein, R.; Dijkstra, K.; Nicolay, K. *Nature* **1978**, *274*, 293.
- (2) Kobori, Y.; Norris, J. R. *J. Am. Chem. Soc.* **2006**, *128*, 4.
- (3) Henbest, K. B.; Maeda, K.; Hore, P. J.; Joshi, M.; Bacher, A.; Bittl, R.; Weber, S.; Timmel, C. R.; Schleicher, E. *Proc. Natl. Acad. Sci. U.S.A.* **2008**, *105*, 14395.
- (4) Mohtat, N.; Cozens, F. L.; Hancock-Chen, T.; Scaiano, J. C.; McLean, J.; Kim, J. *Photochem. Photobiol.* **1998**, *67*, 111.
- (5) Miura, T.; Maeda, K.; Arai, T. *J. Phys. Chem. B* **2003**, *107*, 6474.
- (6) Kiryutin, A. S.; Morozova, O. B.; Kuhn, L. T.; Yurkovskaya, A. V.; Hore, P. J. *J. Phys. Chem. B* **2007**, *111*, 11221.
- (7) Byrdin, M.; Sartor, V.; Eker, A. P. M.; Vos, M. H.; Aubert, C.; Brettel, K.; Mathis, P. *Biochim. Biophys. Acta* **2004**, *1655*, 64.
- (8) Hore, P. J.; Kaptein, R. *Biochemistry* **1983**, *22*, 1906.
- (9) Steiner, U. E.; Ulrich, T. *Chem. Rev.* **1989**, *89*, 51.
- (10) In fields of this magnitude, the decrease in S–T mixing is caused by an increased Zeeman splitting between the S and T_{\pm} manifolds.
- (11) The $^1\text{AQDS}^{2-}$ reaction with water competes with the molecule's target reaction with the protein but does not show any MFE. For more information and spectra, see the SI.

JA908988U